

Dynamics of the Interaction of Vapor-Deposited Copper with Alkanethiolate Monolayers: Bond Insertion, Complexation, and Penetration Pathways

Gabriella Nagy and Amy V. Walker*

Department of Chemistry and Center for Materials Innovation, Washington University in St. Louis, Campus Box 1134, One Brookings Drive, St. Louis, Missouri 63130

Received: September 6, 2005; In Final Form: April 19, 2006

We have investigated the interaction of vapor-deposited copper with $-\text{CH}_3$, $-\text{OH}$, $-\text{OCH}_3$, $-\text{COOH}$, and $-\text{CO}_2\text{CH}_3$ terminated alkanethiolate self-assembled monolayers (SAMs) adsorbed on polycrystalline Au using time-of-flight secondary ion mass spectrometry and density functional theory calculations. For $-\text{OH}$, $-\text{COOH}$, and $-\text{CO}_2\text{CH}_3$ terminated SAMs measurements indicate that for all copper coverages there is a competition between Cu atom bond insertion into C–O bonds, stabilization at the SAM/vacuum interface, and penetration to the Au/S interface. In contrast, on a $-\text{OCH}_3$ terminated SAM Cu only weakly interacts with the methoxy group and penetrates to the Au substrate, while for a $-\text{CH}_3$ terminated SAM deposited copper only penetrates to the Au/S interface. The insertion of copper into C–O terminal group bonds is an activated process. We estimate that the barriers for Cu insertion are $55 \pm 5 \text{ kJ mol}^{-1}$ for the ester, $50 \pm 5 \text{ kJ mol}^{-1}$ for the acid, and $55 \pm 5 \text{ kJ mol}^{-1}$ for the hydroxyl terminated SAMs. The activation barrier for the copper insertion is much higher for the $-\text{OCH}_3$ SAM. Copper atoms with energies lower than the activation barrier partition between complexation (weak interaction) with the terminal groups and penetration through the monolayer to the Au/S interface. Weakly stabilized copper atoms at the SAM/vacuum interface slowly penetrate through the monolayer. In contrast to the case of Al deposition, C–O bond insertion is favored over C=O, C–H, and C–C bond insertion.

1. Introduction

Understanding and controlling the interaction of metals with thin organic films are critical to many technological applications including polymer light-emitting diodes^{1–3} and organic/molecular electronics.^{4–15} Metallized polymers are also employed in reflectors,¹⁶ food packaging,¹⁷ compact disks,¹⁷ prosthetic implants,¹⁸ microelectronics packaging,^{19,20} and thin film transistors.^{21–24} For example, multilayer structures of polyimides and copper have been used to produce high-density, faster interconnects.¹⁹

The interaction of metals with thin organic films is a complex process and depends on the metal, organic film, deposition method, and experimental conditions. A wide variety of interactions have been observed, from strong chemical reactions^{25,26} in which the structural integrity of the film is destroyed, to metal–organic complex formation,²⁷ to penetration of the metal into the bulk,^{28,29} which can cause electrical shorts. Remarkably, there is still little understanding of the kinetics and the dynamics of metal–organic thin film interactions. The rational design of metal–organic structures requires a fundamental understanding of the chemistry of the metal–molecule interaction, to control how and where metal contacts are created.

Many workers have employed self-assembled monolayers (SAMs) as model systems to study the interaction of metals with thin organic films.^{17,25–35} Self-assembled monolayers have highly organized, well-defined structures and have a uniform density of terminal functional groups, which allows for the quantitative analysis of the metal–molecule interaction. Furthermore, these surfaces can be systematically modified, which allows for the direct comparison of the reactivity of different terminal groups. The use of SAMs in these studies is also

relevant since there is great interest in their use in molecular electronic devices. In these devices, a SAM is formed on either a metallic or a semiconducting substrate, and a top contact is formed by vacuum physical vapor deposition of a metallic contact.³⁶

Since the mid-1990s copper has been employed, rather than Al, as interconnects in microchips³⁷ as well as for wiring.³⁸ However, copper interacts only weakly with polymers leading to inadequate interfacial adhesion and diffusion of Cu into the organic film, which can cause electrical shorts.^{19,20} Thus it is important to understand the reactivity of Cu with functional groups commonly found in polymers, such as $-\text{CH}_3$, $-\text{OH}$, $-\text{OCH}_3$, $-\text{COOH}$, and $-\text{CO}_2\text{CH}_3$. Further, it has been suggested that functionalized SAMs could be employed as both adhesion promoters and diffusion barriers at the Cu– SiO_2 interface for sub-100-nm device production. Recent studies by Ganesan and co-workers increased the Cu-diffusion-induced time-to-failure by a factor of 12 by using a carboxyl terminated SAM as a barrier layer.³⁹ Increases in Cu-diffusion-induced time-to-failure were also observed for pyridine⁴⁰ and phenyl⁴⁰ terminated SAMs.

There have been a number of studies of the interaction of vapor-deposited copper on functionalized alkanethiolate SAMs.^{28,30,32,34,41–44} To date no clear trends in the reactivity of vapor-deposited copper with $-\text{CH}_3$, $-\text{OH}$, $-\text{OCH}_3$, $-\text{COOH}$, and $-\text{CO}_2\text{CH}_3$ terminated SAMs have been determined. The interaction of Cu with $-\text{CO}_2\text{CH}_3$ terminal groups has been studied by Allara and co-workers using infrared spectroscopy (IRS), X-ray photoelectron spectroscopy (XPS), and scanning tunneling microscopy (STM).³⁰ From the IRS data, they concluded that Cu inserts into the O– CH_3 bond of the terminal group and that deposited Cu clusters at the SAM/vacuum

interface, in agreement with observations made using STM. However, the XPS data showed that there was only a weak interaction between the vapor-deposited copper and the terminal group. In later XPS experiments, Herdt and Czanderna⁴¹ observed that there was no Cu/–CO₂CH₃ interaction. There was some indirect evidence that Cu interacted with the terminal group since it was observed using ion scattering spectroscopy (ISS) that Cu penetrated through a –CO₂CH₃ terminated SAM more slowly than through a –CH₃ terminated SAM.⁴¹ For the Cu/–OCH₃ interaction, Walker et al. observed that copper does not insert into the O–CH₃ bond but rather weakly interacted with the terminal group and penetrated through the monolayer to the Au/S interface at all coverages studied.^{28,32,34} Using XPS, Czanderna and co-workers showed that vapor-deposited Cu reacted with –OH⁴² and –COOH⁴³ terminated SAMs by inserting into the C–O bond to form a Cu(I) complex. The XPS data also suggested that Cu penetrates through the –OH terminated SAM.⁴² However, using IRS, XPS, and atomic force microscopy (AFM) measurements Smith et al. concluded that Cu formed a Cu(II) carboxylate with an acid terminated alkanethiolate SAM.⁴⁴ Later experiments by Czanderna and co-workers using XPS and ISS also concluded that copper formed a Cu(II) complex with the terminal group and penetrated through the SAM to the Au/S interface.⁴³

In this paper we investigate the dynamics of the interaction of vapor-deposited Cu on –CH₃, –OH, –OCH₃, –COOH, and –CO₂CH₃ terminated SAMs using time-of-flight secondary ion mass spectrometry (TOF SIMS) and density functional theory (DFT) theory calculations. For all the monolayers studied we observe that vapor-deposited copper penetrates through the SAM to the Au/S interface. For –OH, –COOH and –CO₂CH₃ terminated SAMs we demonstrate that copper also interacts with the terminal group in two ways: (a) It inserts into C–O bonds to form a stable metal–organic complex, and (b) it weakly interacts with the terminal group and is stabilized at the SAM/vacuum interface. For the –OCH₃ terminated SAM, in agreement with Walker et al.,^{28,34} we observe that Cu does not insert into C–O bonds but rather interacts weakly with the terminal group and is stabilized at the SAM/vacuum interface. These observations indicate that insertion of Cu into C–O bonds is an activated process and that the energetic barrier for Cu insertion into the –OCH₃ terminal moiety is prohibitively high. We estimate the barrier for insertion of Cu into the –OH, –COOH, and –CO₂CH₃ terminal groups to be 55 ± 5 , 50 ± 5 , and 55 ± 5 kJ mol^{–1}, respectively. Furthermore we show that between 80% and 90% of the vapor-deposited Cu remains at the SAM/vacuum interface. Our data also indicate that vapor-deposited Cu forms islands on these SAM surfaces and that no continuous metallic overlayer forms for any coverage studied.

2. Experimental Section

2.1. Materials and Sample Preparation. The materials for all metal depositions were obtained from Alfa Aesar, Inc., and were of 99.995% purity.

The preparation and characterization of the SAMs used in this study have been described in detail previously.^{27,31,32,45} Briefly, Cr (~10 nm) and Au (~100–200 nm) were sequentially thermally deposited onto clean Si native oxide covered wafers (<111>, Addison Technology, Inc.). Self-assembly of well-organized monolayers was achieved by immersing the Au substrates into a 1 mmol solution of the relevant hexadecanethiol molecule (with –CH₃, –COOH, –CO₂CH₃, –OCH₃, or –OH terminal functional groups) (obtained from Professor D. L. Allara, Pennsylvania State University) in absolute ethanol (Aaper

Alcohol and Chemical Co.) for 24 h at ambient temperature (21 ± 2 °C). To ensure that the SAMs were well-ordered and that there was no significant chemical contamination, the monolayers were characterized by single-wavelength ellipsometry (Gaertner, Inc.) and TOF SIMS prior to copper deposition.

2.2. Time-of-Flight Secondary Ion Mass Spectrometry. Time-of-flight secondary ion mass spectrometry analyses were performed using a TOF SIMS IV (ION TOF, Inc.). Briefly, the instrument consists of a loadlock, a preparation/metal-deposition chamber, and an analysis chamber, each separated by a gate valve. The primary Au⁺ ions were accelerated to 25 keV and contained in a 150 nm diameter probe beam, which was rastered over a $(100 \times 100) \mu\text{m}^2$ area during data acquisition. All spectra were acquired in the static SIMS regime using a total ion dose of less than 10^9 ions cm^{–2}. The secondary ions generated were extracted into a time-of-flight mass spectrometer and reaccelerated to 10 keV before reaching the detector. Relative peak intensities were reproducible to within $\pm 10\%$ from sample to sample and $\pm 8\%$ from scan to scan.

Copper was thermally deposited onto a room-temperature sample from a tungsten-wire basket at a rate of ~ 0.6 atoms nm^{–2} s^{–1}, with the preparation chamber pressure maintained below 5×10^{-8} mbar. After deposition, the preparation chamber pressure was allowed to recover to the base pressure (1×10^{-9} mbar) before sample transfer to the analysis chamber. The deposited mass per unit area was monitored using a quartz crystal microbalance (QCM; TM-400 controller, Maxtek, Inc.; deposition accuracy $\pm 8\%$). For each copper deposition at least two samples were prepared, and three areas on each sample were examined.

2.3. Quantum Mechanical Calculations. Density functional theory geometry optimization calculations were performed to provide estimates of the interaction energy of copper with –OH, –OCH₃, –COOH, and –CO₂CH₃ terminated SAMs. The calculations were carried out using the NWChem 4.5 program package⁴⁶ at the PW91PW91/LANL2DZ(Au,Cu)/cc-pVDZ (S,C,O,H) level of theory. To reduce the computational cost the SAM was truncated to 10 methylene units and modeled as T–(CH₂)₅–SAu, where T = –OH, –OCH₃, –COOH, and –CO₂CH₃. The missing subunits are not expected to significantly affect the calculated bond energies since intramolecular induction effects typically have a range of 2–3 C–C bonds.

2.4. Definition of Deposited Copper Coverage. The copper deposition was directly monitored using a QCM. To aid data analysis and interpretation, all deposited amounts were converted to coverage of copper atoms per SAM molecule, θ_{Cu} . The molecular density is 4.6 molecules nm^{–2} in a well-formed alkanethiolate SAM on Au{111}.⁴⁷ We assume that the sticking probability of copper is unity on the SAM surfaces. Thus the number of copper atoms deposited was calculated using its density (8.96 g cm^{–3}),⁴⁸ its average atomic mass (63.54(3) Da),⁴⁸ and the film thickness recorded by the QCM.

3. Results

The results for the deposition of Cu on –OCH₃ terminated SAMs have been reported previously by Walker et al.^{28,34} and are included here for comparison purposes. Table 1 summarizes the fragment and cluster ions observed in the TOF SIMS spectra upon vapor deposition of copper on –CH₃, –OCH₃, –CO₂CH₃, –OH, and –COOH terminated SAMs.

3.1. Bare Monolayer. The positive and negative secondary ion mass spectra of the bare –CH₃, –OCH₃, –CO₂CH₃, –OH, and –COOH terminated alkanethiolate monolayers adsorbed on gold have been discussed in detail previously.^{27,28,31,32,34,35,49}

TABLE 1: Fragment and Cluster Observed in the TOF SIMS Spectra upon Copper Deposition on $-\text{CH}_3$, $-\text{OCH}_3$, $-\text{OH}$, $-\text{COOH}$, and $-\text{CO}_2\text{CH}_3$ Terminated SAMs

terminal group	fragment ions
$-\text{CH}_3$	Cu_x^+ ($x = 1-3$), CuSH_2^+ , $\text{CuS}(\text{CH}_2)_x^+$, $\text{Au}_x\text{Cu}_y\text{S}_z^{\pm}$
$-\text{OCH}_3$	CuOCH_3^+ , Cu_x^+ ($x = 1-3$), CuSH_2^+ , $\text{CuS}(\text{CH}_2)_x^+$, $\text{Au}_x\text{Cu}_y\text{S}_z^{\pm}$
$-\text{OH}$	$\text{Cu}_x\text{O}_y^{\pm}$, CuOC^+ , $\text{CuO}(\text{CH}_2)_x^{\pm}$, CuOH^+ , $\text{CuOH}(\text{CH}_2)_x^+$, $\text{CuO}(\text{CH})_x(\text{CH}_2)_y^+$, Cu_x^+ ($x = 1-3$), CuSH_2^+ , $\text{CuS}(\text{CH}_2)_x^+$, $\text{Au}_x\text{Cu}_y\text{S}_z^{\pm}$
$-\text{COOH}$	$\text{Cu}_x\text{O}_y^{\pm}$, CuOC^+ , $\text{CuOC}(\text{CH}_2)_x^{\pm}$, $\text{CuO}_2\text{C}(\text{CH}_2)_x^+$, $[(\text{CH})(\text{COOH})\text{Cu}]^+$, Cu_x^+ ($x = 1-3$), CuSH_2^+ , $\text{CuS}(\text{CH}_2)_x^+$, $\text{Au}_x\text{Cu}_y\text{S}_z^{\pm}$
$-\text{CO}_2\text{CH}_3$	$\text{Cu}_x\text{O}_y^{\pm}$, CuOC^+ , $\text{CuOC}(\text{CH}_2)_x^{\pm}$, $\text{CuO}_2\text{C}(\text{CH}_2)_x^+$, $[(\text{CH})(\text{COOH})\text{Cu}]^+$, CuOCH_3^+ , CuOH^+ , Cu_x^+ ($x = 1-3$), CuSH_2^+ , $\text{CuS}(\text{CH}_2)_x^+$, $\text{Au}_x\text{Cu}_y\text{S}_z^{\pm}$

In agreement with earlier results we observe that the intensities of SO_x^- ($x = 1-4$) and Au_yS_z^- provide useful information that the SAM was prepared without substantial incorporation of impurities and was not oxidized.

3.2. Penetration of Copper to the Au/S Interface. Upon deposition of copper, for all monolayers studied, we observe the formation of CuSH_x^+ , $\text{Au}_x\text{Cu}_y\text{S}_z^{\pm}$, and $\text{CuS}(\text{CH}_2)_x^+$ ions indicating that copper has penetrated to the Au/S interface. Figure 1 displays the intensity of CuSH_2^+ ($m/z = 97$) for increasing increments of copper deposition upon the $-\text{CH}_3$, $-\text{OCH}_3$, $-\text{CO}_2\text{CH}_3$, $-\text{OH}$, and $-\text{COOH}$ terminated SAMs. The CuSH_2^+ peak intensity is normalized to the peak intensity of $\text{C}_7\text{H}_{13}^+$ to make clear the change in peak intensities with respect to the hydrocarbon fragments. The intensity of the CuSH_2^+ ion increases throughout the deposition indicating that Cu penetrates through the monolayer at all Cu coverages studied. We also observe similar behavior for both the $\text{Au}_x\text{Cu}_y\text{S}_z^{\pm}$ and the $\text{CuS}(\text{CH}_2)_x^+$ ion intensities (data not shown).

Another important indicator that Cu penetrates through these SAMs is the relatively constant intensity of the Au_2A^- peaks, which involve intact adsorbed molecules (A). Figure 2 shows the intensity of the Au_2A^- ion upon copper deposition on the $-\text{CH}_3$, $-\text{OCH}_3$, $-\text{CO}_2\text{CH}_3$, $-\text{OH}$, and $-\text{COOH}$ terminated SAMs. The Au_2A^- intensities barely drop below their initial values for $\theta_{\text{Cu}} \leq 46$ suggesting that the SAM molecules are left chemically intact after Cu deposition. The molecular ion intensity, in fact, increases upon Cu deposition, which is probably due to electron transfer from the more electropositive deposited Cu atoms to the more electronegative Au atoms and clusters leaving the surface.³¹ Consistent with the approximately constant molecular ion intensities during the initial stages of the copper deposition the hydrocarbon fragment and Au-containing cluster ion intensities also remain approximately unchanged. At higher coverages ($\theta_{\text{Cu}} > 46$), all peak intensities for the $-\text{OH}$, $-\text{OCH}_3$, and $-\text{CO}_2\text{CH}_3$ terminated SAMs become attenuated suggesting that a metal overlayer, which can block ion ejection from the substrate, is forming. The attenuation of the molecular cluster ions is much faster for the $-\text{COOH}$ terminated SAM. At $\theta_{\text{Cu}} = 46$ for the $-\text{COOH}$ terminated SAM, the intensity of the Au_2A^- ion has decreased to within the noise of the mass spectrum (Figure 2d).

Further information about the state of the penetrated Cu atoms is given by the intensities of the Cu^+ , Cu_2^+ , and Cu_3^+ ions. In Figure 3 it can clearly be seen that the dimer (Cu_2^+) and trimer (Cu_3^+) ion intensities increase proportionately with the first increment of deposited Cu on the $-\text{OCH}_3$, $-\text{OH}$, $-\text{COOH}$, and $-\text{CO}_2\text{CH}_3$ terminated SAMs. Recently, Allara, Winograd, and co-workers demonstrated that metal cluster ion intensities differ

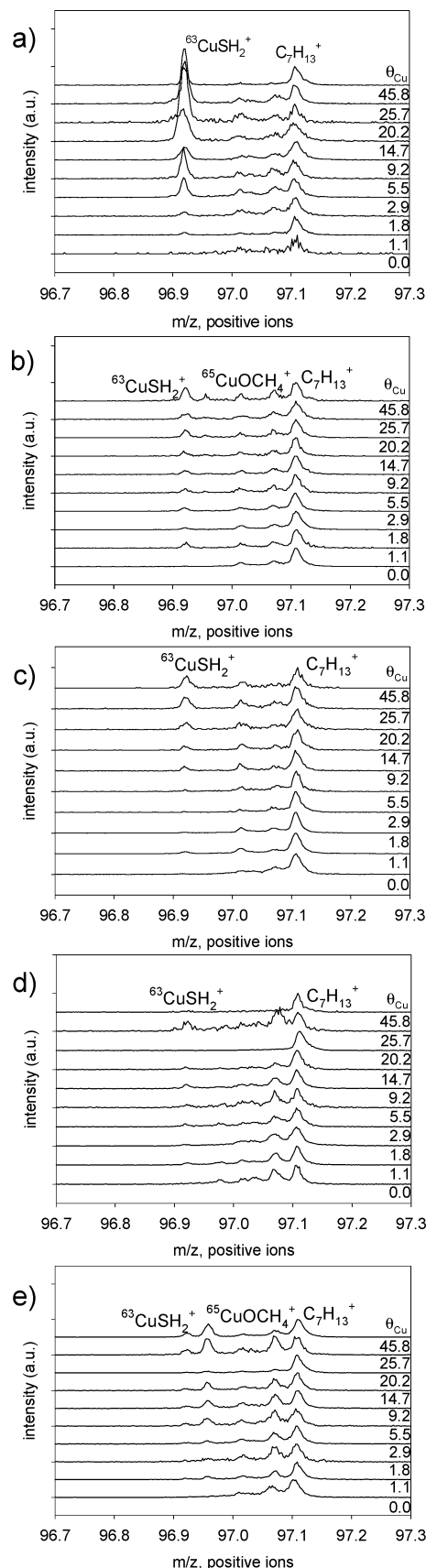


Figure 1. High-resolution positive ion mass spectra of $^{63}\text{CuSH}_2^+$ fragments (nominal mass $m/z = 97$) for increasing increments of Cu deposited on (a) $-\text{CH}_3$, (b) $-\text{OCH}_3$, (c) $-\text{OH}$, (d) $-\text{COOH}$, and (e) $-\text{CO}_2\text{CH}_3$ terminated SAMs. The intensities in the plots are normalized to the initial peak intensity of $\text{C}_7\text{H}_{13}^+$ to make clear the changes in the SIMS spectra upon Cu deposition.

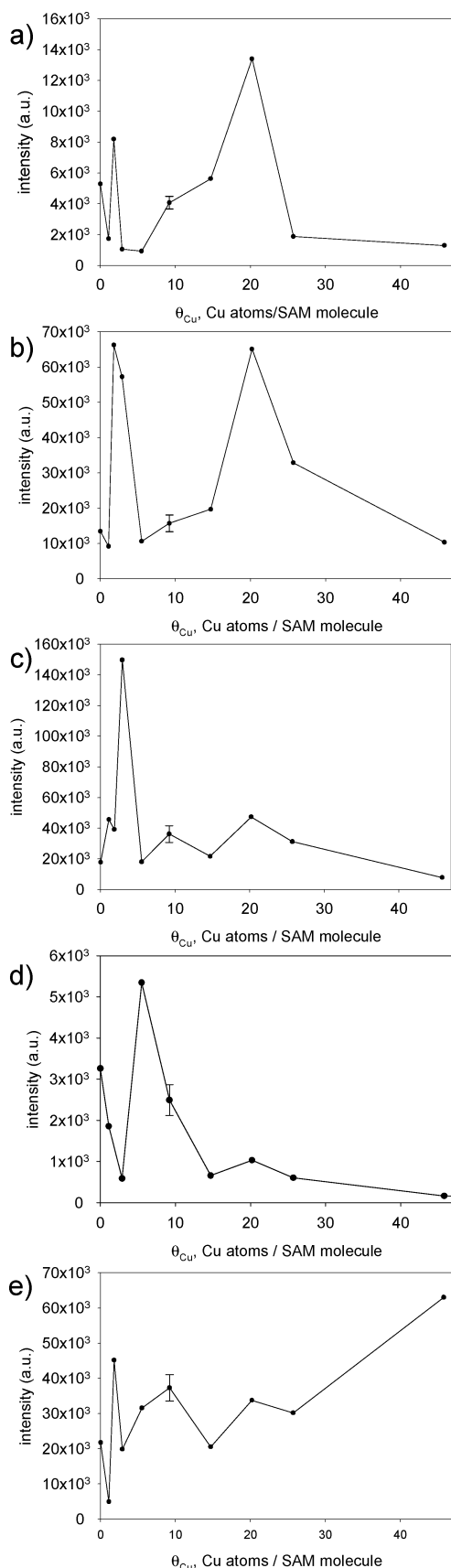


Figure 2. Integrated SIMS molecular ion peak intensities of Au_2A^- plotted vs copper coverage for (a) $-\text{CH}_3$, (b) $-\text{OCH}_3$, (c) $-\text{OH}$, (d) $-\text{COOH}$, and (e) $-\text{CO}_2\text{CH}_3$ terminated SAMs. The single error bar shown in each plot is representative of the uncertainty for each datum.

between systems where vapor-deposited metal penetrates through the monolayer to the Au/S interface and where it chemisorbs

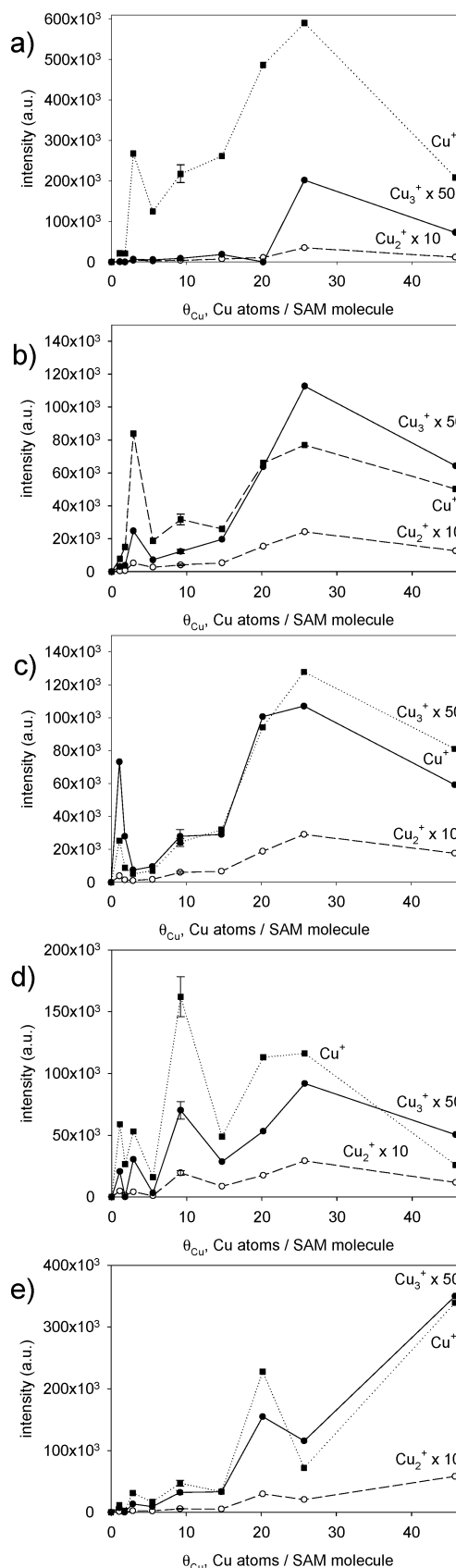


Figure 3. Integrated SIMS ion peak intensities of $^{63}\text{Cu}^+$, $^{63}\text{Cu}_2^+$, and $^{63}\text{Cu}_3^+$ plotted vs copper coverage for (a) $-\text{CH}_3$, (b) $-\text{OCH}_3$, (c) $-\text{OH}$, (d) $-\text{COOH}$, and (e) $-\text{CO}_2\text{CH}_3$ terminated SAMs. The single error bar shown in each plot is representative of the uncertainty for each datum.

at the SAM/vacuum interface.^{27,28,31,32} For Cu deposition on $-\text{OCH}_3$ terminated SAMs, Walker et al.²⁸ observed that the

Cu_2^+ and Cu_3^+ ion intensities increase proportionately with the first increment of deposited metal. This study concluded that Cu penetrates through the SAM as well as weakly interacts with the $-\text{OCH}_3$ terminated SAM. This suggests that vapor-deposited Cu both reacts with the $-\text{OH}$, $-\text{COOH}$, and $-\text{CO}_2\text{CH}_3$ terminal groups and penetrates through these SAMs to the Au/S interface. In contrast, for the $-\text{CH}_3$ terminated SAM the Cu^+ and Cu_2^+ ion intensities increase steadily while there is a slight delay in the growth of the Cu_3^+ ion intensity (Figure 3). Similar behavior was observed for the vapor deposition of Al on $-\text{CH}_3$ terminated SAMs³¹ where the first increments of Al penetrate through the monolayer to the Au/S interface and the Al^+ and Al_2^+ ion signals increase steadily while there is a slight delay in the growth of the Al_3^+ ion intensity. Together with the other ions observed (Table 1), these observations indicate that vapor-deposited copper penetrates through the methyl terminated SAM and does not interact with the terminal group.

3.3. Reaction of Deposited Cu with $-\text{OH}$, $-\text{COOH}$, $-\text{OCH}_3$, and $-\text{CO}_2\text{CH}_3$ Terminal Groups. Both the positive and the negative ion TOF SIMS mass spectra indicate that vapor-deposited Cu interacts with the $-\text{OH}$, $-\text{COOH}$, $-\text{OCH}_3$, and $-\text{CO}_2\text{CH}_3$ terminal groups. In agreement with previous work,^{28,34} upon Cu deposition on $-\text{OCH}_3$ terminated SAMs we observe the formation of CuOCH_3^+ ions but not $\text{Cu}_x\text{O}_y^{\pm}$ ions, indicating that Cu has not inserted into the C–O bond of the terminal group. Rather, the presence of the CuOCH_3^+ ion indicates that deposited copper atoms weakly interact with the methoxy terminal group and are stabilized at the SAM/vacuum interface.^{28,34} In contrast, for $-\text{OH}$, $-\text{COOH}$, and $-\text{CO}_2\text{CH}_3$ terminated SAMs, $\text{Cu}_x\text{O}_y^{\pm}$ ions such as CuO^+ are observed to form, indicating that vapor-deposited Cu has undergone an insertion reaction with these terminal groups (Figure 4). Other metal–organic ions that indicate that Cu interacts with these terminal groups are given in Table 1 and Figure 5. There are several ions that indicate that some of the oxygen atoms in the $-\text{OH}$, $-\text{COOH}$, and $-\text{CO}_2\text{CH}_3$ terminal groups remain unreacted. For example, upon vapor deposition of Cu on $-\text{OH}$ terminated SAMs we observe the formation of $\text{Cu}(\text{OH})(\text{CH}_2)^+$, while in the $-\text{CO}_2\text{CH}_3$ and $-\text{COOH}$ terminated SAM mass spectra we observe ions of the form $[(\text{CH})(\text{COOH})\text{Cu}]^+$. The persistence of these ions indicates that some of the functional groups remain intact throughout the deposition regime.^{27,31} However, it is not clear in the case of the $-\text{CO}_2\text{CH}_3$ and $-\text{COOH}$ terminated SAMs whether the oxygen atoms are in the hydroxyl or carboxyl form. Upon Cu deposition on $-\text{CO}_2\text{CH}_3$ terminated SAMs, CuOCH_3^+ ions are also observed to form. Ions of this type were not observed in previous studies of Al vapor deposition on $-\text{CO}_2\text{CH}_3$ terminated SAMs³¹ and suggest that there may be a weak interaction between the deposited Cu atoms and the ester functional group. Similarly, for Cu deposited on $-\text{COOH}$ and $-\text{OH}$ terminated SAMs we observed ions of the form CuOH^{\pm} . Ions of this type were also not observed in previous studies of Al deposition on $-\text{COOH}$ ²⁷ and $-\text{OH}$ ³² terminated SAMs. This indicates that there may also be a weak interaction between the vapor-deposited Cu and these functional groups.

We can determine the relative strength of a copper–organic interaction by following the intensity of the characteristic fragment ions with time. If the fragment ion intensities decrease significantly, then it suggests that copper atoms are slowly diffusing to the Au/S interface and that the copper–organic interaction is weak. In contrast, if copper has inserted into the SAM terminal group, then we expect that the fragment ion intensity would remain approximately constant with time. To

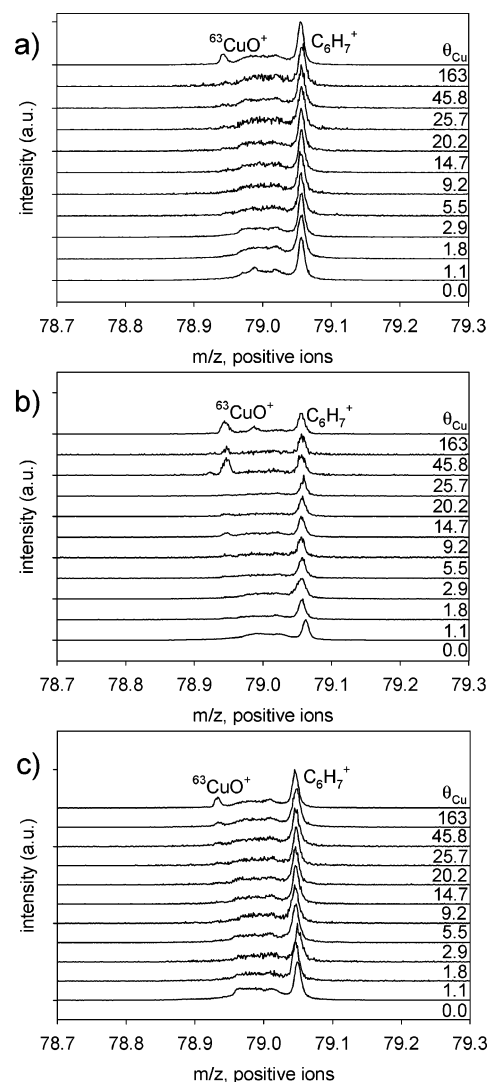


Figure 4. High-resolution positive ion mass spectra of $^{63}\text{CuO}^+$ fragments (nominal mass $m/z = 79$) for increasing increments of deposited copper on (a) $-\text{OH}$, (b) $-\text{COOH}$, and (c) $-\text{CO}_2\text{CH}_3$ terminated SAMs. The intensities in the plots are normalized to the initial peak intensity of C_6H_7^+ to make clear the changes in the SIMS spectra upon Cu deposition.

test this hypothesis we deposited $\theta_{\text{Cu}} = 46$ (25 Å) on a $-\text{OCH}_3$ terminated SAM and followed the intensities of the CuOCH_3^+ (indicative of the weak Cu–terminal group interaction) and CuSH_2^+ (indicative of the penetration of Cu to the Au/S interface) with time.^{28,34} The experiment was performed in the following way. Copper was vapor-deposited simultaneously on 10 separate $-\text{OCH}_3$ terminated SAM samples. At certain times after deposition, positive and negative TOF SIMS spectra were obtained. A different sample was used at each time point to ensure that there were no changes induced in the sample by the primary ion beam. All samples were kept under vacuum ($<5 \times 10^{-9}$ mbar) after copper deposition. In Figure 6 it can clearly be seen that the intensity of the CuOCH_3^+ ion decreases significantly, indicating that Cu is leaving the SAM/vacuum interface and penetrating through the SAM to the Au/S interface. After 2580 min (43 h) the intensity of the CuOCH_3^+ ion is $\sim 20\%$ of its original value. However, we also note that the CuSH_2^+ ion intensity has not increased during this time and, in fact, has decreased to $\sim 70\%$ of its original value (Figure 6). There are two possible explanations for a decrease in the CuOCH_3^+ ion intensity while the CuSH_2^+ intensity remains approximately constant: (a) Cu has desorbed from the SAM

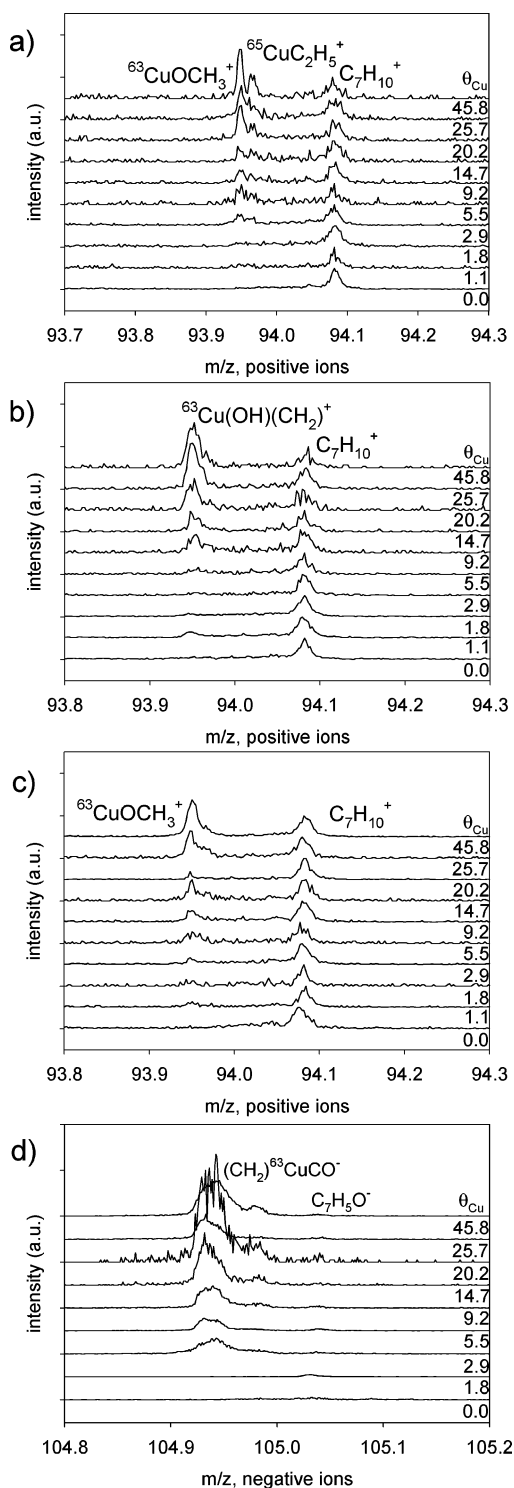


Figure 5. High-resolution SIMS mass spectra of (a) $^{63}\text{CuOCH}_3^+$ (nominal mass $m/z = 94$), (b) $^{63}\text{Cu(OH)(CH}_2)^+$ (nominal mass $m/z = 94$), (c) $(\text{CH}_2)^{63}\text{CuCO}^-$ (nominal mass $m/z = 105$), and (d) $^{63}\text{CuOCH}_3^+$ (nominal mass $m/z = 94$) for copper deposition upon (a) $-\text{OCH}_3$, (b) $-\text{OH}$, (c) $-\text{COOH}$, and (d) $-\text{CO}_2\text{CH}_3$ terminated SAMs, respectively. The intensities in plots a, b, and d are normalized to the initial peak intensity of $\text{C}_7\text{H}_{10}^+$ to make clear the changes in the SIMS spectra upon Cu deposition. In plot c, the intensity of $(\text{CH}_2)^{63}\text{CuCO}^-$ is normalized to the initial peak intensity of $\text{C}_7\text{H}_5\text{O}^-$ to make clear the changes in the SIMS spectra upon Cu deposition.

surface into the vacuum, and (b) Cu has penetrated through the monolayer to the Au/S interface and diffused into the Au substrate. It is unlikely that Cu has desorbed from the SAM/vacuum interface since the Cu_x^+ , Au_xCu_y^+ , and $\text{Au}_x\text{Cu}_y\text{S}_z^\pm$ ion intensities remain approximately constant throughout the experi-

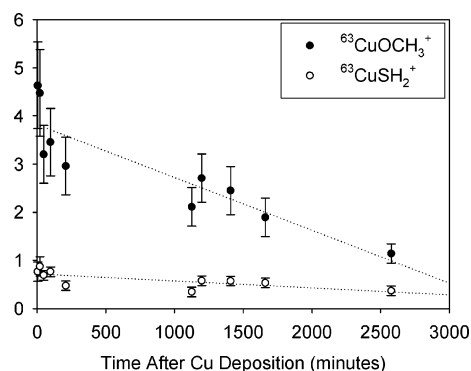


Figure 6. Integrated SIMS ion peak intensities of $^{63}\text{CuOCH}_3^+$ and $^{63}\text{CuSH}_2^+$ plotted vs time after deposition of $\theta_{\text{Cu}} = 46$ ML upon $-\text{OCH}_3$ terminated SAMs. The intensities of the $^{63}\text{CuOCH}_3^+$ and $^{63}\text{CuSH}_2^+$ ions are normalized to the initial peak intensities of $\text{C}_7\text{H}_{13}^+$ and $\text{C}_7\text{H}_{10}^+$ to make clear the changes in the SIMS spectra upon Cu vapor deposition.

ment. Furthermore, ISS experiments indicate that vapor-deposited Cu penetrates slowly through the monolayer to the Au/S interface after deposition.^{41,50} Thus we conclude that the total amount of copper remains constant on the SAM and that Cu atoms slowly penetrate to the Au/S interface and diffuse into the Au substrate.

Figure 7 shows the variation of copper–organic ion intensities after deposition of $\theta_{\text{Cu}} = 46$ (25 Å) on $-\text{CO}_2\text{CH}_3$, $-\text{COOH}$, and $-\text{OH}$ terminated SAMs with time. The experiments were performed in a manner similar to that described for the $-\text{OCH}_3$ terminated SAM. We observe that the intensities of the CuOC^+ and CuSH_2^+ ions retain 70–75% of their original intensity. The relatively constant CuOC^+ ion intensities indicate that these ions arise from insertion of Cu atoms into the Cu–O bonds of the $-\text{OH}$, $-\text{COOH}$, and $-\text{CO}_2\text{CH}_3$ terminated SAMs. We also observe Cu- and O-containing ions whose intensities decrease significantly with time. The intensity of the $\text{Cu(OH)(CH}_2)^+$ ion decreases after Cu deposition on $-\text{OH}$ terminated SAMs; after 2700 min the $\text{Cu(OH)(CH}_2)^+$ ion intensity is $\sim 33\%$ of its initial value (Figure 7a). Similarly, for acid terminated SAMs, we observe that the $[(\text{CH}_2)\text{COCu}]^-$ ion intensity decreases to $\sim 44\%$ of its initial value after 1725 min (Figure 7b). For the $-\text{CO}_2\text{CH}_3$ terminated SAM, the intensity of the CuOCH_3^+ ion decreases with time. After 2700 min, the CuOCH_3^+ ion intensity is $\sim 40\%$ of its original value (Figure 7c). The significant decrease of intensity for all these ions with time suggests that there are also weak interactions between the vapor-deposited copper and the $-\text{CO}_2\text{CH}_3$, $-\text{OH}$, and $-\text{COOH}$ terminated SAMs, stabilizing Cu atoms at the SAM/vacuum interface.

4. Discussion

There have been many studies of the interactions of vapor-deposited metals with functionalized SAMs, which are briefly summarized here. In general, the following behaviors have been observed: (a) destruction of the monolayer with inorganic compound formation (e.g., Ti or Ca deposited on $-\text{OCH}_3$ terminated SAMs²⁶), (b) reaction with the terminal group to form metal–organic complexes (e.g., Al deposited on $-\text{CO}_2\text{CH}_3$,³¹ $-\text{COOH}$,²⁷ and $-\text{OH}$ ³² terminated SAMs), (c) weak interaction with the terminal group stabilizing the metal atoms at the SAM/vacuum interface (e.g., Al, Cu, and Ag deposition on $-\text{OCH}_3$ terminated SAMs^{28,32,34}), (d) penetration of the metal atoms to the Au/S interface (e.g., Au deposited on molecular wire SAMs²⁵), and (e) a combination of these processes.^{28,32,34} Finally, the formation of a metallic overlayer is governed by the strength of the metal–metal bonding and the metal–SAM molecule interaction.

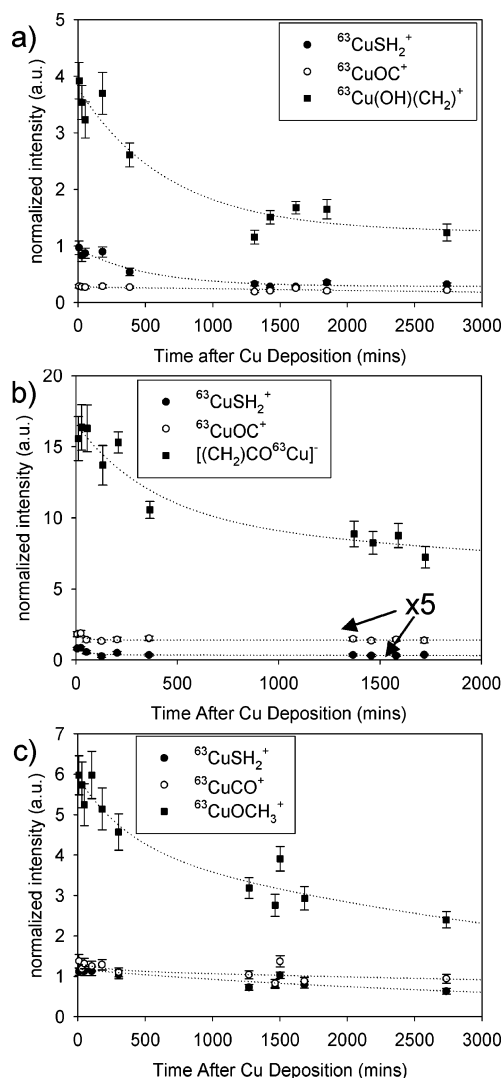


Figure 7. Integrated SIMS ion peak intensities of various oxygen-containing ions, $^{63}\text{CuOC}^+$, and CuSH_2^+ plotted vs time after deposition of $\theta_{\text{Cu}} = 46$ ML upon (a) $-\text{OH}$, (b) $-\text{COOH}$, and (c) $-\text{CO}_2\text{CH}_3$ terminated SAMs. The intensities of the $^{63}\text{CuOC}^+$, $^{63}\text{CuSH}_2^+$, $^{63}\text{Cu}(\text{OH})(\text{CH}_2)^+$, $[(\text{CH}_2)\text{CO}^{63}\text{Cu}]^+$, and $^{63}\text{CuOCH}_3^+$ ions are normalized to the initial peak intensities of C_7H_7^+ , $\text{C}_7\text{H}_{13}^+$, $\text{C}_7\text{H}_{10}^+$, $\text{C}_5\text{H}_{13}\text{S}^+$, and $\text{C}_7\text{H}_{10}^+$, respectively, to make clear the changes in the SIMS spectra upon Cu deposition. The dotted lines are shown as a guide to the eye.

Figure 8 gives a schematic summary of the interaction of vapor-deposited Cu with $-\text{CH}_3$, $-\text{OH}$, $-\text{OCH}_3$, $-\text{COOH}$, and $-\text{CO}_2\text{CH}_3$ terminated SAMs. Briefly, Cu penetrates through all the monolayers studied. On the $-\text{CO}_2\text{CH}_3$, $-\text{OH}$, and $-\text{COOH}$ terminated SAMs, Cu also interacts with the terminal group in two ways: (a) insertion into the terminal moiety and (b) a weak interaction in which Cu is stabilized at the SAM/vacuum interface (complexation). For $-\text{OCH}_3$ terminated SAMs, vapor-deposited Cu also interacts weakly (complexes) with the methoxy group and is stabilized at the SAM/vacuum interface. A summary of the reaction pathways is given below

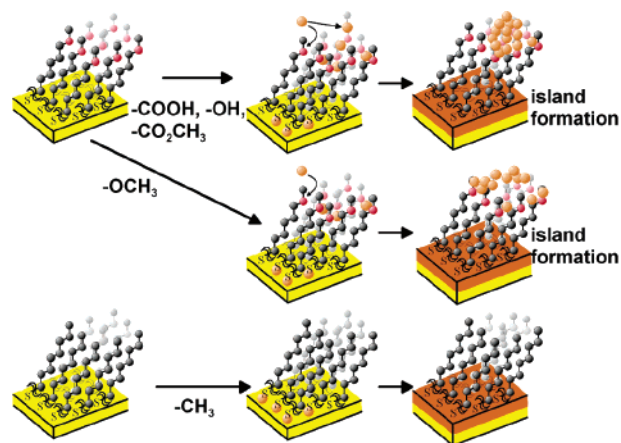
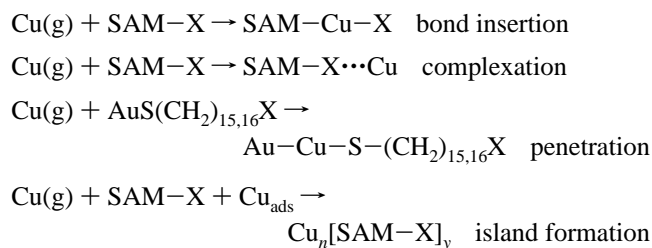


Figure 8. Schematic illustrations of the important features of the reaction pathways observed upon copper deposition on $-\text{CH}_3$, $-\text{OCH}_3$, $-\text{OH}$, $-\text{COOH}$, and $-\text{CO}_2\text{CH}_3$ terminated SAMs. The copper atoms are represented in orange, gold in yellow, oxygen in red, and hydrocarbons in black.

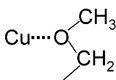
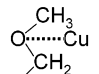
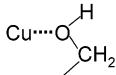
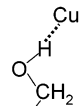
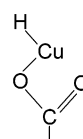
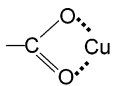
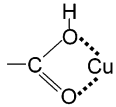
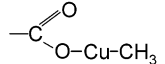
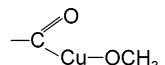
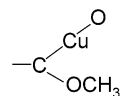
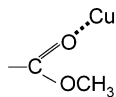
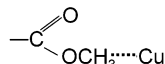
The reactivity of the vapor-deposited copper is determined by its kinetic energy and the competition between chemical bond insertion, complexation, and penetration to the Au/S interface and island formation. We shall discuss each of these processes in turn.

4.1. Reaction of Vapor-Deposited Cu with $-\text{OCH}_3$, $-\text{CO}_2\text{CH}_3$, $-\text{COOH}$, and $-\text{OH}$ Terminal Groups. **4.1.1. Copper Insertion Reactions.** In the mass spectrum of vapor-deposited Cu on $-\text{CO}_2\text{CH}_3$, $-\text{COOH}$, and $-\text{OH}$ terminated SAMs, we observe the formation on $\text{Cu}_x\text{O}_y^\pm$ ions, which indicates that Cu has inserted into these terminal groups. For $-\text{OCH}_3$ terminated SAMs, copper does not insert into the methoxy group. To aid in the determination of the structure of these metal-organic complexes, we performed DFT calculations of the interaction of Cu with gas-phase $\text{AuS}(\text{CH}_2)_5\text{X}$ where $\text{X} = -\text{CO}_2\text{CH}_3$, $-\text{COOH}$, $-\text{OH}$, and $-\text{OCH}_3$. The results are summarized in Table 2.

For the ester terminated SAM, the most stable state at -132 kJ mol^{-1} occurs when the Cu atom inserts into the $\text{O}-\text{CH}_3$ bond, in agreement with the experimental results of Allara et al.³⁰ Using Fourier transform reflection/absorption IRS, they observed that upon Cu vapor deposition on a $-\text{CO}_2\text{CH}_3$ terminated SAM two new vibrational modes at 1406 and 1666 cm^{-1} appeared, which they assigned to an asymmetric Cu(I) carboxylate formed by insertion of Cu into the $\text{O}-\text{CH}_3$ bond of the terminal group. Our DFT calculations show that insertion of Cu into the $\text{C}-\text{OCH}_3$ bond is calculated to be stable by only -0.2 kJ mol^{-1} and so this structure is unlikely to form. Our calculations also show that insertion of Cu into the $\text{C}=\text{O}$ bond of the $-\text{CO}_2\text{CH}_3$ SAM is unstable. We note that the most stable structure for the $-\text{OCH}_3$ terminated SAM is the insertion of Cu into the $\text{O}-\text{CH}_3$ bond of the terminal group, -39 kJ mol^{-1} . However, this reaction is not experimentally observed suggesting that the energy barrier for the insertion process is prohibitively high.^{28,34}

The energy minimum for both the $-\text{COOH}$ and the $-\text{OH}$ terminated SAMs is the insertion of Cu into the $\text{C}-\text{OH}$ bond, stable by -65 and -36 kJ mol^{-1} respectively, in agreement with previous XPS data. Czanderna and co-workers concluded from the O 1s and Cu $2p_{3/2}$ XPS spectra that for both $-\text{OH}$ ⁴² and $-\text{COOH}$ ⁴³ terminated SAMs Cu inserts into the $\text{C}-\text{OH}$ bond, forming a Cu(I)-O unidentate complex. However, using IRS and XPS, Smith et al.⁴⁴ concluded that for $-\text{COOH}$ terminated SAMs vapor-deposited Cu reacts with the $-\text{COOH}$

TABLE 2: Calculated Stabilization Energies for Various Complexes

Terminal Group	Reaction	Complex Structure	Stabilization Energy (kJ mol ⁻¹)
-OCH ₃	insertion into H ₂ C-OCH ₃	H ₂ C-Cu-OCH ₃	-39.2
	insertion into (CH ₂)O-CH ₃	(CH ₂) ₂ O-Cu-CH ₃	-16.4
	complexation		-14.5
	complexation		-3.0
-OH	insertion into H ₂ C-OH	H ₂ C-Cu-OH	-36.2
	insertion into (CH ₂)O-H	(CH ₂) ₂ O-Cu-H	+40.3; unstable
	complexation		-18.7
	complexation		-7.6
-COOH	insertion into CH ₂ CO(O-H)		-65.1
	complexation		+148.1; unstable
	complexation		-32.6
-CO ₂ CH ₃	insertion into C(O)O-CH ₃		-132.3
	insertion into (O)C-OCH ₃		-0.2
	insertion into (CH ₃ O)C-O		+6.9; unstable
	complexation		-17.8
	complexation		-2.1

terminal group to form a Cu(II) carboxylate salt rather than a Cu(I) pseudoester. Later XPS and X-ray excited Auger electron spectroscopy (XAES) studies by Czanderna and co-workers concluded that Cu forms a complex oxide in the +2 valence state, possibly with some OH character.⁵⁰ No Cu²⁺ shake-up peaks were observed in the XPS spectra,⁵⁰ suggesting that the maximum charge on the copper atoms in the Cu-O complex is +1.

4.1.2. Stabilization of Cu at the SAM/Vacuum Interface. The presence of ions in the TOF SIMS spectra whose intensities change significantly with time demonstrates that there is a stabilizing interaction between the Cu and the -OCH₃, -COOH, -OH, and -CO₂CH₃ terminal groups but not an insertion into a C-O bond. Further evidence that a fraction of the vapor-deposited Cu does not insert into the terminal group is obtained from XPS, IRS, and ISS data. For the -OCH₃ terminated SAM,

Walker et al.²⁸ using IRS observed that the character of the C–O stretch mode at 1132 cm⁻¹ was nearly constant. Using XPS and ISS Herdt and Czanderna⁴¹ observed that vapor-deposited Cu interacts weakly with –CO₂CH₃ terminal groups leading to the stabilization of Cu at the SAM/vacuum interface. For –OH⁴² and –COOH^{43,50} terminated SAMs, XPS data indicate that copper interacts with the terminal groups but does not form a +1 or +2 oxide, which may indicate that there is a weak interaction between the deposited Cu and the terminal group (see ref 28 and references therein). We note that this interaction is strong enough to localize copper atoms at the SAM/vacuum interface leading to the nucleation and growth of a metallic overlayer (islands) but is weak enough that the penetration of copper through the monolayer remains competitive.

To further investigate this weak interaction between the vapor-deposited Cu atoms and the functionalized SAMs, we employed DFT calculations. Secondary minima are found in which copper atoms interact with the intact –OCH₃, –CO₂CH₃, –COOH, and –OH terminal groups (Table 2). For the ester terminated SAM, there are two secondary minima; there is a structure stable by –17.8 kJ mol⁻¹ in which the copper atom is closely associated with the carbonyl cluster (forming a C=O...Cu unidentate structure) and a less stable structure (stable by –2.1 kJ mol⁻¹) in which the Cu atom associates with the CH₃ group of the –OCH₃ moiety. For the –COOH terminated SAM, Cu forms a weakly bound structure, stable by –32.6 kJ mol⁻¹, by interacting with both oxygen atoms of the acid terminal group. For the –OH and –OCH₃ terminated SAMs, there are secondary minima, stable by –18.8 and –14.5 kJ mol⁻¹, respectively, in which the Cu atom associates with the O atom of the terminal group.

4.2. Formation of a Metallic Overlayer and Penetration of Cu to the Au/S Interface. For all the SAMs studied, at $\theta_{\text{Cu}} = 163$ (189 Å) we observe ions that originate from the monolayer, indicating that vapor-deposited Cu does not form a continuous metallic overlayer at the SAM/vacuum interface. However, the signals from the –CO₂CH₃, –COOH, –OH, and –OCH₃ terminated SAMs are attenuated, suggesting that a metallic overlayer is forming on some parts of the vacuum/SAM surface. There is some evidence in the TOF SIMS mass spectra that vapor-deposited copper forms islands at the SAM/vacuum interface: The ion intensities of Cu₂⁺ and Cu₃⁺ ions increase continually over the deposition range for all the monolayers studied, which suggests that Cu deposits as clusters and islands. There is further evidence of Cu island formation from STM and AFM measurements.^{30,44} Jeon and Allara³⁰ observed that after deposition of 6.5 Å (12 ML) of Cu on a –CO₂CH₃ terminated SAM the copper forms elongated islands with lateral dimensions of approximately (14 × 36) nm² and thickness ~2 nm. This implies that only ~33% of the SAM surface is covered by the Cu film if all the copper adsorbed at the SAM/vacuum interface. Smith et al.⁴⁴ examined the structure of copper islands formed after deposition of 50 Å (92 ML) of Cu on a –COOH terminated SAM. These AFM measurements revealed that the copper islands were approximately 20 nm in length, which was considerably smaller than the crystallite structure of the underlying Au surface.

To try to quantify the amount of copper that penetrates through the SAM, we examined the intensities of the CuSH₂⁺ signals upon increasing Cu deposition. By comparing the CuSH₂⁺ ion intensities from the –CH₃ terminated and functionalized SAMs, we can calculate the amount of copper that remains at the SAM/vacuum interface. We note that secondary ion intensities are dependent upon the matrix that surrounds

the structure of interest, and thus quantitation is relatively difficult. There are two approaches to quantify SIMS ion intensities: relative sensitivity factors⁵¹ and use of an internal standard.⁵² We have combined the two approaches to obtain the fraction of copper at the SAM/vacuum interface for the –OCH₃, –OH, –COOH, and –CO₂CH₃ terminated SAMs. If we assume that if all the vapor-deposited Cu penetrates through the –CH₃ terminated SAM, then the relative concentration of the penetrated Cu atoms for the functionalized SAMs, $C_{\text{p, funct. SAM}}$, is given by

$$C_{\text{p, funct. SAM}} = \text{RSF} \frac{I_{\text{CuSH}_2^+} C_{\text{methyl chain}}}{I_{\text{C}_7\text{H}_{13}^+}}$$

where RSF is the relative sensitivity factor, $I_{\text{CuSH}_2^+}$ is the intensity of the CuSH₂⁺ ion, $C_{\text{methyl chain}}$ is the concentration of the SAM methylene chains, and $I_{\text{C}_7\text{H}_{13}^+}$ is the intensity of C₇H₁₃⁺ ions (which arise from the methylene backbone of the SAMs). Similarly, the concentration (fraction) of penetrated copper through the methyl terminated SAM, $C_{\text{p, -CH}_3 \text{ SAM}}$, is given by

$$C_{\text{p, -CH}_3 \text{ SAM}} = \text{RSF} \frac{I_{\text{CuSH}_2^+} C_{\text{methyl chain}}}{I_{\text{C}_7\text{H}_{13}^+}}$$

If we assume that all the vapor-deposited copper penetrates through the –CH₃ terminated SAM at room temperature, then

$$\text{RSF} = \left(\frac{I_{\text{C}_7\text{H}_{13}^+}}{I_{\text{CuSH}_2^+} C_{\text{methyl chain}}} \right)_{\text{-CH}_3 \text{ terminated SAM}}$$

At low copper coverages ($\theta_{\text{Cu}} \leq 25$) the assumption that Cu only penetrates through the –CH₃ terminated SAM is reasonable since the hydrocarbon fragment and Au-containing cluster ion intensities are only slightly attenuated (or even increase) upon copper deposition, indicating that little or no metal overlayer forms at the SAM/vacuum interface. Herdt and co-workers^{41,53} also observed using XPS and ISS that most vapor-deposited Cu penetrates through –CH₃ terminated SAMs. Since the environment of the penetrated copper atoms at low coverages is similar for all the SAMs studied, the relative fraction of Cu at the Au/S interface is given by

$$\begin{aligned} C_{\text{p, funct. SAM}} &= \left(\frac{I_{\text{C}_7\text{H}_{13}^+}}{I_{\text{CuSH}_2^+} C_{\text{methyl chain}}} \right)_{\text{-CH}_3 \text{ terminated SAM}} \left(\frac{I_{\text{CuSH}_2^+} C_{\text{methyl chain}}}{I_{\text{C}_7\text{H}_{13}^+}} \right) \\ &= \left(\frac{I_{\text{C}_7\text{H}_{13}^+}}{I_{\text{CuSH}_2^+}} \right)_{\text{-CH}_3 \text{ terminated SAM}} \left(\frac{I_{\text{CuSH}_2^+}}{I_{\text{C}_7\text{H}_{13}^+}} \right) \end{aligned}$$

(We note that at high copper coverages there will be significant changes in the matrix (environment) at the Au/S interface. This may lead to significant changes in the ionization cross section.) The fraction of the vapor-deposited Cu at the SAM/vacuum interface, f , is therefore given by

$$f = 1 - C_{\text{p, funct. SAM}}$$

Figure 9 displays the fraction of vapor-deposited copper at the SAM/vacuum interface estimated using the above method. At $\theta_{\text{Cu}} \leq 5$, the percentage of copper that is present at the SAM/vacuum interface varies from 20% to 70%. At higher coverages ~80–90% of the copper deposited is present at the SAM/

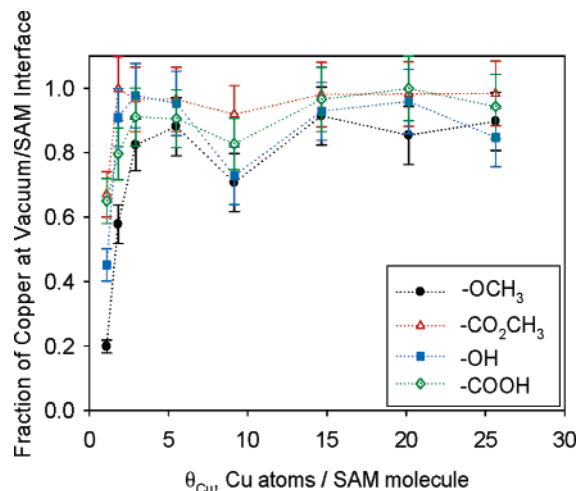


Figure 9. Fraction of vapor-deposited copper at the SAM/vacuum interface plotted vs θ_{Cu} for $-OCH_3$, $-OH$, $-COOH$, and $-CO_2CH_3$ terminated SAMs. The dotted lines are shown as a guide to the eye.

vacuum interface. These observations suggest that copper is forming islands at the SAM/vacuum interface in agreement with the STM and AFM observations.^{30,44}

4.3. Energetics. A satisfactory model describing the reaction of vapor-deposited copper with SAMs must be able to explain why Cu atoms (a) insert into $-COOH$, $-CO_2CH_3$, and $-OH$ terminated SAMs but not $-OCH_3$ SAMs, (b) weakly interact with $-OCH_3$, $-COOH$, $-CO_2CH_3$, and $-OH$ terminated SAMs, and (c) penetrates to the Au/S interface.

For $-CO_2CH_3$, $-COOH$, and $-OH$ terminated SAMs, we observe that a fraction of the deposited Cu atoms inserts into the C–O bonds of the terminal groups, while another fraction weakly interacts (complex) with the terminal group, which stabilizes them at the SAM/vacuum interface. In contrast, for $-OCH_3$ terminated SAMs the complexation reaction is observed, but Cu insertion into the O–CH₃ bond is not. Using DFT calculations we have demonstrated that the insertion of Cu–O atoms into the C–O bonds of these terminal groups, including $-OCH_3$ terminated SAMs, is the thermodynamically favored process. However, we also observe that Cu weakly interacts with these terminal groups. This suggests that there is a large activation barrier for the insertion of Cu atoms into the C–O bond, which in the case of the methoxy group is prohibitively high. We can estimate the height of the barrier for the insertion reaction of Cu into the $-CO_2CH_3$, $-OH$, and $-COOH$ terminal groups in the following way. For all three SAMs, the intensity of the $CuOC^+$ ion increases throughout the deposition (Figure 10) and reaches a maximum at $\theta_{Cu} \approx 100$ –160 ML. This suggests that at this coverage the insertion reaction has saturated; one Cu atom has reacted with each terminal group. In Figure 10, it can clearly be seen that the intensity of the $CuOC^+$ ion increases rapidly between $\theta_{Cu} = 0$ and 5 ML, suggesting that the activation barrier for Cu insertion is lower at low coverages than that at high coverages, possibly due to blocking of unreacted terminal groups by the Cu adlayer. The initial rapid reaction of copper with $-OH$ and $-COOH$ terminated SAMs was also observed by Czanderna and co-workers using XPS.^{42,43} For 11-mercaptoundecanol SAMs, Jung and co-workers⁴² concluded that a large fraction of the hydroxyl groups had reacted by $\theta_{Cu} \approx 1.8$ –9 ML (1–5 Å). In the case of 11-mercaptoundecanoic acid monolayers the copper–SAM interaction was observed to be saturated between $\theta_{Cu} \approx 3$ and 11 (2–6 Å).⁴³ We also note that in both these studies it was concluded that one Cu atom reacted with each terminal group.

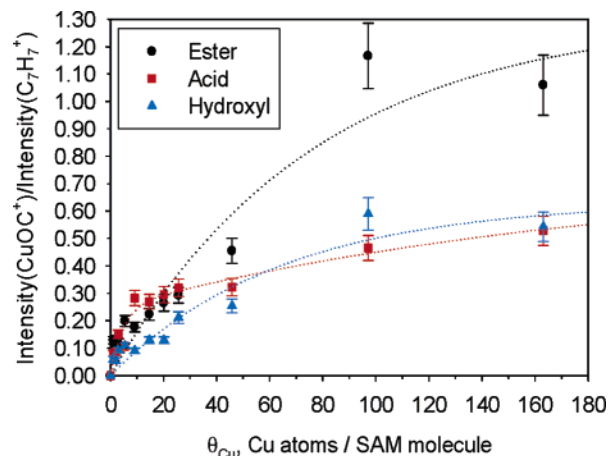


Figure 10. Integrated SIMS ion peak intensities of $^{63}CuOC^+$ plotted vs θ_{Cu} for $-OH$, $-COOH$, and $-CO_2CH_3$ terminated SAMs. The intensities of the $^{63}CuOC^+$ ions are normalized to the $C_7H_7^+$ integrated peak intensity to make clear the changes in the mass spectra upon Cu deposition. The dotted lines are shown as a guide to the eye.

We can estimate initial reaction probabilities for Cu insertion in the following way. The reaction probability is given by the ratio of copper atoms reacted to the total number deposited. If one Cu atom inserts into the terminal group,^{42,43} then the fraction of Cu atoms that undergo insertion into the C–O bond can be calculated from the intensity of the $CuOC^+$ ions in the following way

$$\text{fraction of Cu atoms reacted} = \frac{\text{intensity of } CuOC^+ \text{ ion}}{\text{intensity of } CuOC^+ \text{ ion for completed reaction}}$$

The reaction probability was calculated using the intensity of the $CuOC^+$ ions after deposition of $\theta_{Cu} = 5$

$$\begin{aligned} \text{reaction probability} &= \frac{\text{fraction of Cu atoms reacted after deposition of } \theta_{Cu} = 5}{\text{total coverage of Cu } (\theta_{Cu} = 5)} \\ &= 0.034 \pm 0.005 \quad -CO_2CH_3 \text{ terminated SAM} \\ &= 0.035 \pm 0.005 \quad -OH \text{ terminated SAM} \\ &= 0.050 \pm 0.005 \quad -COOH \text{ terminated SAM} \end{aligned}$$

In an oven source, metal atoms are generated with a Maxwell distribution of velocities. If every copper atom with sufficient energy to overcome the activation barrier inserts into the C–O bond of the terminal group, then

$$\begin{aligned} \int_u^\infty P(v) dv &= 0.034 \pm 0.005 \quad -CO_2CH_3 \text{ terminated SAM} \\ &= 0.035 \pm 0.005 \quad -OH \text{ terminated SAM} \\ &= 0.050 \pm 0.005 \quad -COOH \text{ terminated SAM} \\ &= \int_u^\infty 4\pi \left(\frac{M}{2\pi RT} \right)^{3/2} v^2 \exp\left(\frac{-Mv^2}{2RT} \right) dv \end{aligned}$$

where $P(v) dv$ is the probability of finding an atom with speed between v and dv , M is the mass of the Cu atom, R is the gas constant, T is the temperature of the source, and u is the speed corresponding to the reaction barrier, E_a , where $E_a = \frac{1}{2}mu^2$.

The temperature of the copper source can be estimated from the Cu vapor pressure, $\sim 5 \times 10^{-8}$ mbar, and is approximately 995–1060 K.⁵⁴ Using these parameters, we estimate that the activation barriers for Cu insertion are 55 ± 5 kJ mol⁻¹ for the ester, 50 ± 5 kJ mol⁻¹ for the acid, and 55 ± 5 kJ mol⁻¹ for the hydroxyl terminated SAMs. The initial activation barrier for Cu insertion may be lower than the average value reported here. At $\theta_{\text{Cu}} = 1$, using the above method the reaction probability for insertion of Cu into the C–O bonds is ~ 0.08 for the ester, ~ 0.08 for the hydroxyl, and ~ 0.15 for the acid terminated SAMs, respectively. Using these parameters, we obtain an activation barrier of 40 ± 5 kJ mol⁻¹.

Cu atoms with energies below the activation barrier partition between overlayer island nucleation, complexation with no bond breaking (stabilization at the SAM/vacuum interface), and penetration to the Au/S interface. The degree of partitioning between overlayer nucleation/complexation and penetration is controlled by the strength of the copper complexation. The mechanism of metal atom penetration has been discussed in detail by Walker et al. (see ref 28 and references therein). Briefly, metal atom penetration occurs via hopping (thermally activated translational motion) of metal–alkanethiolate complexes, which leads to the appearance of transient defects in the monolayer. These defects are sufficiently large to allow diffusion of metal atoms to the Au/S interface.

The stabilization of copper at the SAM/vacuum interface is controlled by the strength of the Cu complexation interaction. While DFT studies (section 4.1.2 and Table 2) of the isolated Cu–alkanethiol molecule complexes indicate that the interaction is relatively strong we note that the energy of this interaction is not entirely clear. For $-\text{OCH}_3$ and $-\text{OH}$ terminated SAMs, copper prefers to interact with the O atom away from the C–O–C bonds. For the $-\text{CO}_2\text{CH}_3$ terminated SAM, Cu primarily interacts with the O atom of the C=O bond and points away from the other oxygen. In contrast, Cu interacts with both oxygens of the $-\text{COOH}$ terminal group. Geometric considerations suggest that all these cluster geometries are unfavorable in the monolayers due to steric hindrances at the SAM/vacuum interface. While a small number of terminal groups may be able to reorient themselves to the optimal geometry for metal–molecule complexation, most will not be able to reorient due to the SAM molecular packing. Thus the stabilization (complexation) energy will be reduced relative to the isolated geometry used to calculate these energies.

4.4. Comparison of Reactivities of $-\text{CH}_3$, $-\text{OCH}_3$, $-\text{CO}_2\text{CH}_3$, $-\text{OH}$, and $-\text{COOH}$. In this paper we have investigated the reactivity of $-\text{CH}_3$, $-\text{OH}$, $-\text{OCH}_3$, $-\text{COOH}$, and $-\text{CO}_2\text{CH}_3$ terminated SAMs upon vapor deposition of Cu. Since the $-\text{COOH}$ and $-\text{CO}_2\text{CH}_3$ SAMs can be viewed as combinations of the $-\text{CH}_3$, $-\text{OH}$, $-\text{OCH}_3$, and $-\text{C=O}$ moieties, we can investigate the reactivity of these moieties toward Cu and the effect of their environment on this reactivity. The $-\text{OH}$, $-\text{COOH}$, and $-\text{CO}_2\text{CH}_3$ groups undergo Cu bond insertion into the $-\text{C}-\text{OH}$, $-\text{C}-\text{OH}$, and $-\text{O}-\text{CH}_3$ bonds, respectively. Neither $-\text{OCH}_3$ or $-\text{CH}_3$ reacts with Cu atoms. Thus it appears that C–O bond attack is favored over C=O, C–H, and C–C bond insertion. However, the dominant interaction of vapor-deposited Cu with the $-\text{OH}$, $-\text{OCH}_3$, $-\text{COOH}$, and $-\text{CO}_2\text{CH}_3$ terminal groups is the stabilization of Cu at the SAM/vacuum interface; there are large energetic barriers to Cu insertion into C–O bonds. This contrasts with Al deposition, where the main process observed is O–H bond insertion for both $-\text{COOH}$ ²⁷ and $-\text{OH}$ ³² terminated SAMs, and C=O bond degradation for the $-\text{CO}_2\text{CH}_3$ terminated SAM.³¹

For Al deposition, C=O bond attack is preferred over C–O, C–C, and C–H insertion, but in the presence of an $-\text{OH}$ moiety the C=O bond is less reactive than the O–H bond.

5. Conclusions

Upon deposition of Cu onto $-\text{CO}_2\text{CH}_3$, $-\text{COOH}$, and $-\text{OH}$ terminated alkanethiolate SAMs, the metal atoms insert into the C–O bonds of the terminal groups, stabilize at the SAM/vacuum interface, forming islands, and penetrate to the Au/S interface. In contrast, for a $-\text{OCH}_3$ terminated SAM Cu does not insert into the terminal group C–O bond but weakly interacts with it, nucleating metallic islands at the vacuum interface, and also penetrates to the Au substrate. In the case of a methyl terminated SAM, vapor-deposited Cu only penetrates to the Au/S interface at all metal coverages studied.

The insertion of copper into C–O terminal group bonds is an activated process. We estimate that the activation barriers for Cu insertion are approximately 55 ± 5 kJ mol⁻¹ for the ester, 50 ± 5 kJ mol⁻¹ for the acid, and 55 ± 5 kJ mol⁻¹ for the $-\text{OH}$ terminated SAMs. Since insertion into the $-\text{O}-\text{CH}_3$ bond is not observed for the $-\text{OCH}_3$ terminated SAM, we conclude that the activation barrier is prohibitively high in this case. However we note that upon deposition of the initial increments of Cu the energetic barrier for insertion may be as low as 40 ± 5 kJ mol⁻¹. Copper atoms with energies lower than the activation barrier partition between complexation (weak interaction) with the terminal groups and penetration through the monolayer to the Au/S interface. In agreement with Czanderna and co-workers,^{41,50} we observe that copper atoms slowly penetrate through the monolayer after cessation of metal deposition.

Finally, for Cu deposition on the SAMs studied C–O bond attack is favored over C=O, C–H, and C–C bond insertion. This is in contrast to Al deposition in which it was observed that C=O bond degradation was favored for $-\text{CO}_2\text{CH}_3$ terminated SAMs³¹ and insertion into the O–H bond was preferred for $-\text{COOH}$ ²⁷ and $-\text{OH}$ ³² terminated SAMs.

The rational design of metal–organic structures requires a fundamental understanding of the chemistry defining the metal–molecule interactions, to control how and where metal contacts are created. By comparing the interaction of different metals with a variety of terminal groups, we are able to gain an understanding of these interactions and use this understanding to rationally design and control many types of metallized organic thin film structures. Experiments are currently underway in our laboratory to investigate the control of these metal–molecule interactions by exploiting their reaction pathways.

Acknowledgment. The authors acknowledge the financial support of a National Science Foundation grant (Grant No. CHE-0518063), an American Chemical Society Petroleum Research Fund Type G grant (Grant No. 38900-G5S), and Washington University in St. Louis start-up funds.

References and Notes

- (1) Halls, J. J. M.; Walsh, C. A.; Greenham, N. C.; Marseglia, E. A.; Friend, R. H.; Moratti, S. C.; Holmes, A. B. *Nature* **1995**, *376*, 498–500.
- (2) Friend, R.; Burroughes, J.; Shimoda, T. *Phys. Today* **1999**, 35–40.
- (3) Kugler, T.; Lögdlund, M.; Salaneck, W. R. *IEEE J. Sel. Top. Quantum Electron.* **1998**, *4*, 14–23.
- (4) Chen, J.; Reed, M. A.; Rawlett, A. M.; Tour, J. M. *Science* **1999**, *286*, 1550–1552.
- (5) Reed, M. A. *Proc. IEEE* **1999**, *87*, 652–658.
- (6) Reed, M. A.; Chen, J.; Rawlett, A. M.; Price, D. W.; Tour, J. M. *Appl. Phys. Lett.* **2001**, *78*, 3735–3737.

- (7) Tour, J. M.; Reinerth, W. A.; Jones, L., II.; Burgin, T. P.; Zhou, C.-W.; Muller, C. J.; Deshpande, M. R.; Reed, M. A. *Ann. N. Y. Acad. Sci.* **1998**, 852, 197–205.
- (8) Collier, C. P.; Mattersteig, G.; Wong, E. W.; Luo, Y.; Beverly, K.; Sampaio, J.; Raymo, F. M.; Stoddart, J. F.; Heath, J. R. *Science* **2000**, 289, 1172–1175.
- (9) Lau, C. N.; Stewart, D. R.; Williams, R. S.; Bockrath, M. *Nano Lett.* **2004**, 4, 569–572.
- (10) Avouris, P. *Acc. Chem. Res.* **2002**, 35, 1026–1034.
- (11) Aviram, A. *J. Am. Chem. Soc.* **1988**, 110, 5687–5692.
- (12) Ratner, M. A.; Davis, B.; Kemp, M.; Mujica, V.; Roitberg, A.; Yaliraki, S. *Ann. N. Y. Acad. Sci.* **1998**, 852, 22–37.
- (13) Metzger, R. M. *Adv. Mater. Opt. Electron.* **1999**, 9, 253–263.
- (14) Metzger, R. M. *Chem. Rev.* **2003**, 103, 3803–3834.
- (15) Metzger, R. M.; Chen, B.; Höpfner, U.; Lakshmikantham, M. V.; Vuillaume, D.; Kawai, T.; Wu, X.; Tachibana, H.; Hughes, T. V.; Sakurai, H.; Baldwin, J. W.; Hosch, C.; Cava, M. P.; Brehmer, L.; Ashwell, G. J. *J. Am. Chem. Soc.* **1997**, 119, 10455–10466.
- (16) *Metallized Plastics: Fundamentals and Applications*; Mittal, K. L., Ed.; Marcel Dekker: New York, 1997.
- (17) Jung, D. R.; Czanderna, A. W.; Herdt, G. C. In *Polymer Surfaces and Interfaces: Characterization, Modification and Application*; Mittal, K. L., Lee, K.-W., Eds.; VSP: Utrecht, The Netherlands, 1997.
- (18) Bodö, P.; Sundgren, J.-E. *J. Vac. Sci. Technol., A* **1984**, 2, 1498–1502.
- (19) Zaporozhchenko, V.; Strunksus, T.; Behnke, K.; von Bechtolsheim, C.; Kiene, M.; Faupel, F. *J. Adhes. Sci. Technol.* **2000**, 14, 467–490.
- (20) Opila, R. L.; Eng, J., Jr. *Prog. Surf. Sci.* **2002**, 69, 125–163.
- (21) Garnier, F.; Hajlaoui, R.; Yassar, A.; Srivastava, P. *Science* **1994**, 265, 1684–1686.
- (22) Li, X.-C.; Siringhaus, H.; Garnier, F.; Holmes, A. B.; Moratti, S. C.; Feeder, N.; Clegg, W.; Teat, S. J.; Friend, R. H. *J. Am. Chem. Soc.* **1998**, 120, 2206–2207.
- (23) Siringhaus, H.; Tessler, N.; Friend, R. H. *Science* **1998**, 280, 1741–1744.
- (24) Gelinck, G. H.; Geuns, T. C. T.; de Leeuw, D. M. *Appl. Phys. Lett.* **2000**, 77, 1487–1489.
- (25) Walker, A. V.; Tighe, T. B.; Stapleton, J. J.; Haynie, B. C.; Allara, D. L.; Winograd, N. *Appl. Phys. Lett.* **2004**, 84, 4008–4010.
- (26) Walker, A. V.; Tighe, T. B.; Haynie, B. C.; Uppili, S.; Allara, D. L.; Winograd, N. *J. Phys. Chem. B* **2005**, 109, 11263–11272.
- (27) Fisher, G. L.; Hooper, A. E.; Opila, R. L.; Allara, D. L.; Winograd, N. *J. Phys. Chem. B* **2000**, 104, 3267–3273.
- (28) Walker, A. V.; Tighe, T. B.; Cabarcos, O.; Reinard, M. D.; Haynie, B. C.; Uppili, S.; Allara, D. L.; Winograd, N. *J. Am. Chem. Soc.* **2004**, 126, 3954–3963.
- (29) Jung, D. R.; Czanderna, A. W.; Herdt, G. C. *J. Vac. Sci. Technol., A* **1996**, 14, 1779–1787.
- (30) Jung, D. R.; Czanderna, A. W. *Crit. Rev. Solid State* **1994**, 19, 1–54.
- (31) Hooper, A.; Fisher, G. L.; Konstadinidis, K.; Jung, D.; Nguyen, H.; Opila, R.; Collins, R. W.; Winograd, N.; Allara, D. L. *J. Am. Chem. Soc.* **1999**, 121, 8052–8064.
- (32) Fisher, G. L.; Walker, A. V.; Hooper, A. E.; Tighe, T. B.; Bahnck, K. B.; Skriba, H. T.; Reinard, M. D.; Haynie, B. C.; Opila, R. L.; Winograd, N.; Allara, D. L. *J. Am. Chem. Soc.* **2002**, 124, 5528–5541.
- (33) Walker, A. V.; Fisher, G. L.; Hooper, A. E.; Tighe, T.; Opila, R. L.; Winograd, N.; Allara, D. L. In *Metallization of Polymers 2*; Sacher, E., Ed.; Kluwer Academic/Plenum: New York, 2002; pp 117–126.
- (34) Walker, A. V.; Tighe, T. B.; Reinard, M. D.; Haynie, B. C.; Allara, D. L.; Winograd, N. *Chem. Phys. Lett.* **2003**, 369, 615–620.
- (35) Tarlov, M. J. *Langmuir* **1992**, 8, 80–89.
- (36) Allara, D. L.; Dunbar, T. D.; Weiss, P. S.; Bumm, L. A.; Cygan, M. T.; Tour, J. M.; Reinerth, W. A.; Yao, Y.; Kozaki, M.; Jones, L., II. *Ann. N. Y. Acad. Sci.* **1998**, 852, 349–370.
- (37) Monteiro, O. R. *J. Vac. Sci. Technol., A* **1999**, 17, 1094–1097.
- (38) Angelpoulos, M. *IBM J. Res. Dev.* **2001**, 45, 57–75.
- (39) Ganesan, P. G.; Singh, A. P.; Ramanath, G. *Appl. Phys. Lett.* **2004**, 85, 579–581.
- (40) Ganesan, P. G.; Cui, G.; Ellis, A. V.; Kane, R. S.; Ramanath, G. *Mater. Sci. Forum* **2003**, 426–432, 3487–3492.
- (41) Herdt, G. C.; Czanderna, A. W. *J. Vac. Sci. Technol., A* **1997**, 15, 513–519.
- (42) Jung, D. R.; King, D. E.; Czanderna, A. W. *Appl. Surf. Sci.* **1993**, 70/71, 127–132.
- (43) Czanderna, A. W.; King, D. E.; Spaulding, D. *J. Vac. Sci. Technol., A* **1991**, 9, 2607–2613.
- (44) Smith, E. L.; Alves, C. A.; Anderegg, J. W.; Porter, M. D.; Spierko, L. M. *Langmuir* **1992**, 8, 2707–2714.
- (45) Nuzzo, R. G.; Dubois, L. H.; Allara, D. L. *J. Am. Chem. Soc.* **1990**, 112, 558–569.
- (46) Straatsma, T. P.; Aprà, E.; Windus, T. L.; Dupuis, M.; Bylaska, E. J.; de Jong, W.; Hirata, S.; Smith, D. M. A.; Hackler, M.; Pollack, L.; Harrison, R.; Nieplocha, J.; Tipparaju, V.; Krishnan, M.; Brown, E.; Cisneros, G.; Fann, G.; Fruchtl, H.; Garza, J.; Hirao, K.; Kendall, R.; Nichols, J.; Tsemekhan, K.; Valiev, M.; Wolinski, K.; Anchell, J.; Bernholdt, D.; Borowski, P.; Clark, T.; Clerc, D.; Daschel, H.; Deegan, M.; Dyall, K.; Elwood, D.; Glendening, E.; Gutowski, M.; Hess, A.; Jaffe, J.; Johnson, B.; Ju, J.; Kobayashi, R.; Kutteh, R.; Lin, Z.; Littlefield, R.; Long, X.; Meng, B.; Nakajima, T.; Niu, S.; Rosing, M.; Sandrone, G.; Stave, M.; Taylor, H.; Thomas, G.; van Lenthe, J.; Wong, A.; Zhang, Z. *NWChem*, version 4.5; Pacific Northwest National Laboratory: Richland, WA, 2003.
- (47) Dubois, L. H.; Nuzzo, R. *Annu. Rev. Phys. Chem.* **1992**, 43, 437–463.
- (48) *CRC Handbook of Chemistry and Physics*, 84th ed.; Lide, D. R., Ed.; CRC Press: Boca Raton, FL 2003.
- (49) Hagenhoff, B.; Benninghoven, A.; Spinke, J.; Liley, M.; Knoll, W. *Langmuir* **1993**, 9, 1622–1624.
- (50) Dake, L. S.; King, D. E.; Czanderna, A. W. *Solid State Sci.* **2002**, 2, 781–789.
- (51) Andersen, C. A.; Hinthorne, J. R. *Anal. Chem.* **1973**, 45, 1421–1438.
- (52) Cornelio, P. A.; Gardella, J. A., Jr. In *Metallization of Polymers*; Sacher, E., Pireaux, J.-J., Kowalczyk, S. P., Eds.; ACS Symposium Series 440; American Chemical Society: Washington, DC, 1990; pp 379–393.
- (53) Herdt, G. C.; King, D. E.; Czanderna, A. W. *Z. Phys. Chem.* **1997**, 202, 163–196.
- (54) Veeco Learning Center—Vapor Pressure Data. http://www.veeco.com/learning/learning_vaporelements.asp (accessed April 19, 2006).